Pergamon

Journal of Structural Geology, Vol. 16, No. 5, pp. 737 to 741, 1994

0191-8141/94 $07.00+0.00

0191-8141(93)E0021-C

Determining the slip vector by graphical construction: use of a simplified representation of the stress tensor

JEAN-FRANÇOIS RITZ

Laboratoire de Géologie Structurale, Université Montpellier II, Place Eugène Bataillon, 34095 Montpellier Cédex 05, France

(*Received* 7 *June* 1993; *accepted in revised form* 17 *November* 1993)

Abstract—A classification of tectonic stress regimes and a simple graphical construction of the slip vector applied on a fault plane are proposed, from a simplified expression of the stress tensor such that its components depend only on the stress ellipsoid shape ratio.

INTRODUCTION

FROM the first theoretical discussions of Wallace (1951) and Bott (1959), the analysis of striated fault planes in terms of tectonic stresses has developed considerably. The determination of stress parameters has two main applications. The first one is the reconstruction of stress patterns at different scales (i.e. trajectories of principal stresses). The second application is the possibility of predicting the direction of movement (slip vector) along a fault plane which is inaccessible to direct observation.

This Short Note presents a classification of tectonic stress states in the upper crust, and a simple graphical method for slip vector construction obtained from a simplified expression of the stress tensor. Requiring only a stereographic diagram, this method is an additional contribution to the determination of the maximum shear stress direction on a given fault plane (see Lisle 1989, Means 1989, Ragan 1990, De Paor 1990, Fleischmann 1992, Fry 1992).

SIMPLIFIED REPRESENTATION OF THE STRESS TENSOR

Mathematical formulation

From an arbitrary tectonic stress tensor displaying a vertical principal stress axis, a simplified tensor can be calculated which only depends on the stress ellipsoid axial ratios, yet preserves the orientation and the sense of the shear stress applied on a fault plane. Following Anderson (1951) it can be supposed that, as a first approximation, one of three principal axes is vertical. This assumption enables us to define three theoretical stress regimes which are extensional (σ_1 vertical), strike-slip (σ_2 vertical) and compressional (σ_3 vertical).

Let **T** be a stress tensor with

$$\mathbf{T}_{ij} = \begin{bmatrix} \sigma_x & 0 & 0 \\ 0 & \sigma_y & 0 \\ 0 & 0 & \sigma_z \end{bmatrix} \quad \text{with } \sigma_x > \sigma_y. \tag{1}$$

σ_x, σ_y and σ_z are principal stresses parallel, respectively, to the three axes **x**, **y** (horizontal) and **z** (vertical) of a Cartesian co-ordinate system. Two operations lead to an expression of the stress tensor depending only on the stress ellipsoid shape ratio ϕ, defined as (Angelier 1975):

$$\phi = \frac{\sigma_2 - \sigma_3}{\sigma_1 - \sigma_3} \quad \text{with} \quad 0 \leq \phi \leq 1. \tag{2}$$

The first operation is the subtraction of an isotropic tensor due to the overburden. The addition or the subtraction of an isotropic tensor does not modify either the direction or the magnitude of the applied shear stress on a fault plane; it only changes the normal stress:

$$\mathbf{T}_{ij}' = \begin{bmatrix} \sigma_x & 0 & 0 \\ 0 & \sigma_y & 0 \\ 0 & 0 & \sigma_z \end{bmatrix} - \begin{bmatrix} \sigma_z & 0 & 0 \\ 0 & \sigma_z & 0 \\ 0 & 0 & \sigma_z \end{bmatrix}$$

$$= \begin{bmatrix} \sigma_x - \sigma_z & 0 & 0 \\ 0 & \sigma_y - \sigma_z & 0 \\ 0 & 0 & 0 \end{bmatrix}. \tag{3}$$

The second operation is the multiplication of this new expression by a scalar $(1/\sigma_1 - \sigma_3)$. The multiplication of

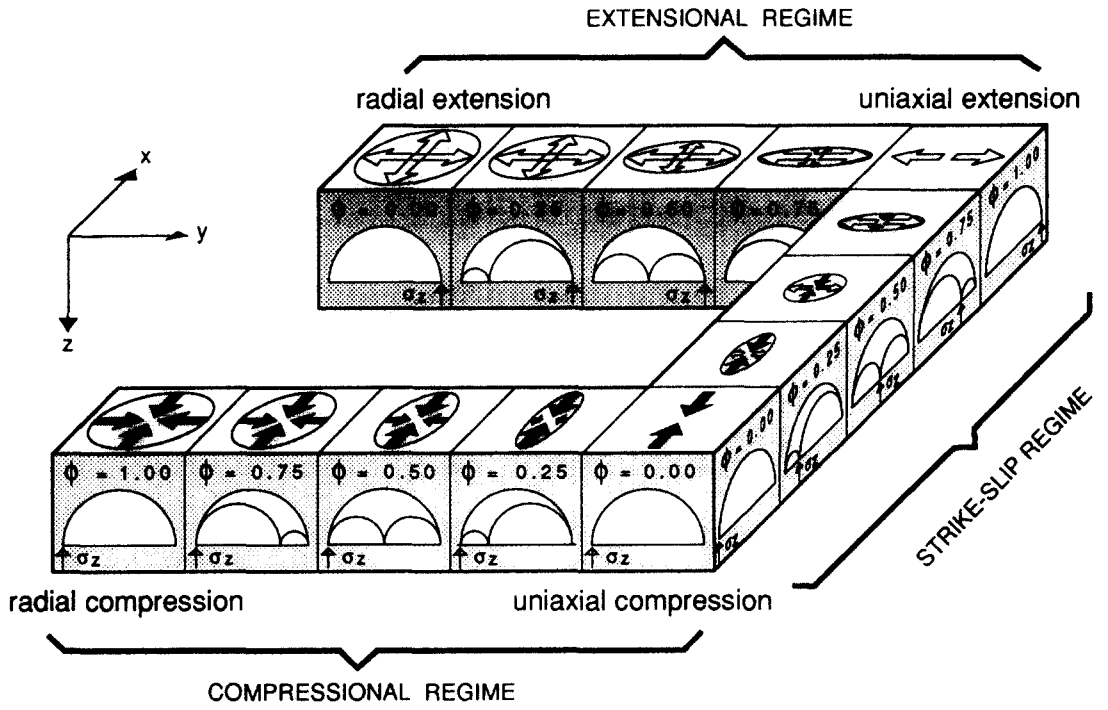

Fig. 1. Classification of the different types of tectonic stress states. Each cube represents a stress tensor which is symbolized by arrows and a Mohr diagram on which σ_z is indicated (see detailed explanations in text).

a tensor by a scalar factor modifies the magnitude of the applied shear stress on a fault plane but not its direction:

$$\mathbf{T}_{ij}'' = \frac{1}{(\sigma_1 - \sigma_3)} \times \begin{bmatrix} \sigma_x - \sigma_z & 0 & 0 \\ 0 & \sigma_y - \sigma_z & 0 \\ 0 & 0 & 0 \end{bmatrix}$$

$$= \begin{bmatrix} \dfrac{\sigma_x - \sigma_z}{\sigma_1 - \sigma_3} & 0 & 0 \\ 0 & \dfrac{\sigma_y - \sigma_z}{\sigma_1 - \sigma_3} & 0 \\ 0 & 0 & 0 \end{bmatrix}. \tag{4}$$

This second operation normalizes the components of the stress tensor with respect to stress difference $(\sigma_1 - \sigma_3)$.

If σ_x, σ_y and σ_z are now replaced by their respective values according to the three stress regimes, the following expressions are obtained.

In an extensional regime $(\sigma_x = \sigma_2, \sigma_y = \sigma_3, \sigma_z = \sigma_1)$

$$\mathbf{T}_{ij}'' = \begin{bmatrix} \dfrac{\sigma_2 - \sigma_1}{\sigma_1 - \sigma_3} & 0 & 0 \\ 0 & \dfrac{\sigma_3 - \sigma_1}{\sigma_1 - \sigma_3} & 0 \\ 0 & 0 & 0 \end{bmatrix}$$

$$= \begin{bmatrix} -(1-\phi) & 0 & 0 \\ 0 & -1 & 0 \\ 0 & 0 & 0 \end{bmatrix}. \tag{5}$$

In a strike-slip regime $(\sigma_x = \sigma_1, \sigma_y = \sigma_3, \sigma_z = \sigma_2)$

$$\mathbf{T}_{ij}'' = \begin{bmatrix} \dfrac{\sigma_1 - \sigma_2}{\sigma_1 - \sigma_3} & 0 & 0 \\ 0 & \dfrac{\sigma_3 - \sigma_2}{\sigma_1 - \sigma_3} & 0 \\ 0 & 0 & 0 \end{bmatrix}$$

$$= \begin{bmatrix} 1-\phi & 0 & 0 \\ 0 & -\phi & 0 \\ 0 & 0 & 0 \end{bmatrix}. \tag{6}$$

In a compressional regime $(\sigma_x = \sigma_1, \sigma_y = \sigma_2, \sigma_z = \sigma_3)$

$$\mathbf{T}_{ij}'' = \begin{bmatrix} \dfrac{\sigma_1 - \sigma_3}{\sigma_1 - \sigma_3} & 0 & 0 \\ 0 & \dfrac{\sigma_2 - \sigma_3}{\sigma_1 - \sigma_3} & 0 \\ 0 & 0 & 0 \end{bmatrix}$$

$$= \begin{bmatrix} 1 & 0 & 0 \\ 0 & \phi & 0 \\ 0 & 0 & 0 \end{bmatrix}. \tag{7}$$

Graphical representation

From these simple expressions, a classification of the different stress states can be presented in one diagram (Fig. 1). Compressional (positive) stresses and extensional (negative) stresses are represented, respectively,

by pairs of convergent black arrows and divergent white arrows. The arrows represent the principal stresses in the reduced expressions of the stress tensor. These stresses can be interpreted as the normalized principal stresses with respect to the difference $(\sigma_1 - \sigma_3)$ at the surface since $\sigma_z = 0$. At the surface, they can be negative (in an extensional regime). At depth, stresses rapidly become compressional whatever the stress state. However, the classification and the representation proposed here can also be applied to describe the stress state at depth, taking into account the following conventions:

(1) it is assumed that one of the three principal stress axes is vertical;

(2) the isotropic stress due to the overburden σ_z is not represented;

(3) stresses greater than σ_z are considered positive;

(4) stresses smaller than σ_z are considered negative.

Figure 1 shows clearly that, for each one of the three different stress regimes, the relative magnitudes of stresses vary continuously. Different stress states are defined by the value of the ϕ ratio (five particular values of ϕ have been chosen to describe this variation: 0.00; 0.25; 0.50; 0.75 and 1.00).

Four particular stress states limit the three main regimes. They correspond to revolution stress ellipsoids around σ_1 (radial extension and uniaxial compression) or σ_3 (radial compression and uniaxial extension) axes.

When the intermediate axis in the simplified expressions is equal to zero (equations 5, 6 and 7), there is a transition from one stress regime to another. There are two possible permutations: between the compressional and the strike-slip regimes (uniaxial compression: $\sigma_2 = \sigma_3$; $\phi = 0$) and between the extensional and strike-slip regimes (uniaxial extension: $\sigma_2 = \sigma_1$; $\phi = 1$).

GRAPHICAL CONSTRUCTION OF THE SLIP VECTORS

From the three expressions of the reduced stress tensor, one can determine using a stereographic projection, the direction of the slip vector on a fault plane whose strike and dip are known. The construction, derived from an unpublished result of Etchecopar (1984), is based on the calculation of the co-ordinates of the resolved *stress vector* **S** applied on the fault plane which depends only on the ϕ value and on the unit vector normal to the fault.

Let **S** be the total stress on a fault plane. **S** is expressed as:

$$\mathbf{S} = \mathbf{T}''\mathbf{n}, \tag{8}$$

where $\mathbf{T}''$ is the reduced stress tensor, and **n** the unit vector perpendicular to the fault, whose co-ordinates are n_x, n_y and n_z in the Cartesian reference frame (x, y, z).

Then, in the three stress regimes, using equations (5), (6), (7) and (8) the coordinates of **S** are the following.

In an extensional regime

$$\mathbf{S}_i = \begin{bmatrix} -(1-\phi)n_x \\ -n_y \\ 0 \end{bmatrix}. \tag{9}$$

In a strike-slip regime

$$\mathbf{S}_i = \begin{bmatrix} (1-\phi)n_x \\ -\phi n_y \\ 0 \end{bmatrix}. \tag{10}$$

In a compressional regime

$$\mathbf{S}_i = \begin{bmatrix} n_x \\ \phi n_y \\ 0 \end{bmatrix}. \tag{11}$$

Notice that the total stress **S** is horizontal in each of the three regimes.

For a graphical determination of the slip vector on a fault plane, four operations are necessary (Fig. 2).

(1) The fault plane and principal stress axes are rotated so that the principal stress axes are parallel to the axes of the co-ordinate system: for the extensional regime, **x**, **y** and **z** are σ_2, σ_3 and σ_1 respectively; for the strike-slip regime **x**, **y** and **z** are σ_1, σ_3 and σ_2, respectively; and for the compressional regime **x**, **y** and **z** are σ_1, σ_2 and σ_3, respectively (Fig. 2, stage 1).

(2) For each fault plane the resolved stress **S** is determined using equations (9), (10) and (11). The vertical component of **S** is zero in all situations, so **S** lies in the horizontal plane. Its location on the stereographic projection is therefore on the exterior circle. To determine **S**, the rotated pole **P'** of the fault plane is projected onto the **x** and **y** horizontal axes to obtain the two components $\mathbf{n_x}'$ and $\mathbf{n_y}'$ which are proportional to $\mathbf{n_x}$ and $\mathbf{n_y}$, respectively (Fig. 2, stage 2). Then, a vector **V**, parallel to **S** is defined, with the following co-ordinates.

In an extensional regime

$$V = \begin{bmatrix} -(1-\phi)n_x' \\ -n_y' \end{bmatrix}. \tag{12}$$

In a strike-slip regime

$$V = \begin{bmatrix} (1-\phi)n_x' \\ -\phi n_y' \end{bmatrix}. \tag{13}$$

In a compressional regime

$$V = \begin{bmatrix} n_x' \\ \phi n_y' \end{bmatrix}. \tag{14}$$

The direction of the resolved stress **S** applied in the fault plane is defined as the intersection between the vector **V** and the exterior circle.

(3) The slip vector τ, which corresponds to the projection of **S** on the fault plane is determined (Fig. 2, stage 3). One only has to find the plane which passes through both **S** and the fault pole, **P**. The intersection of this

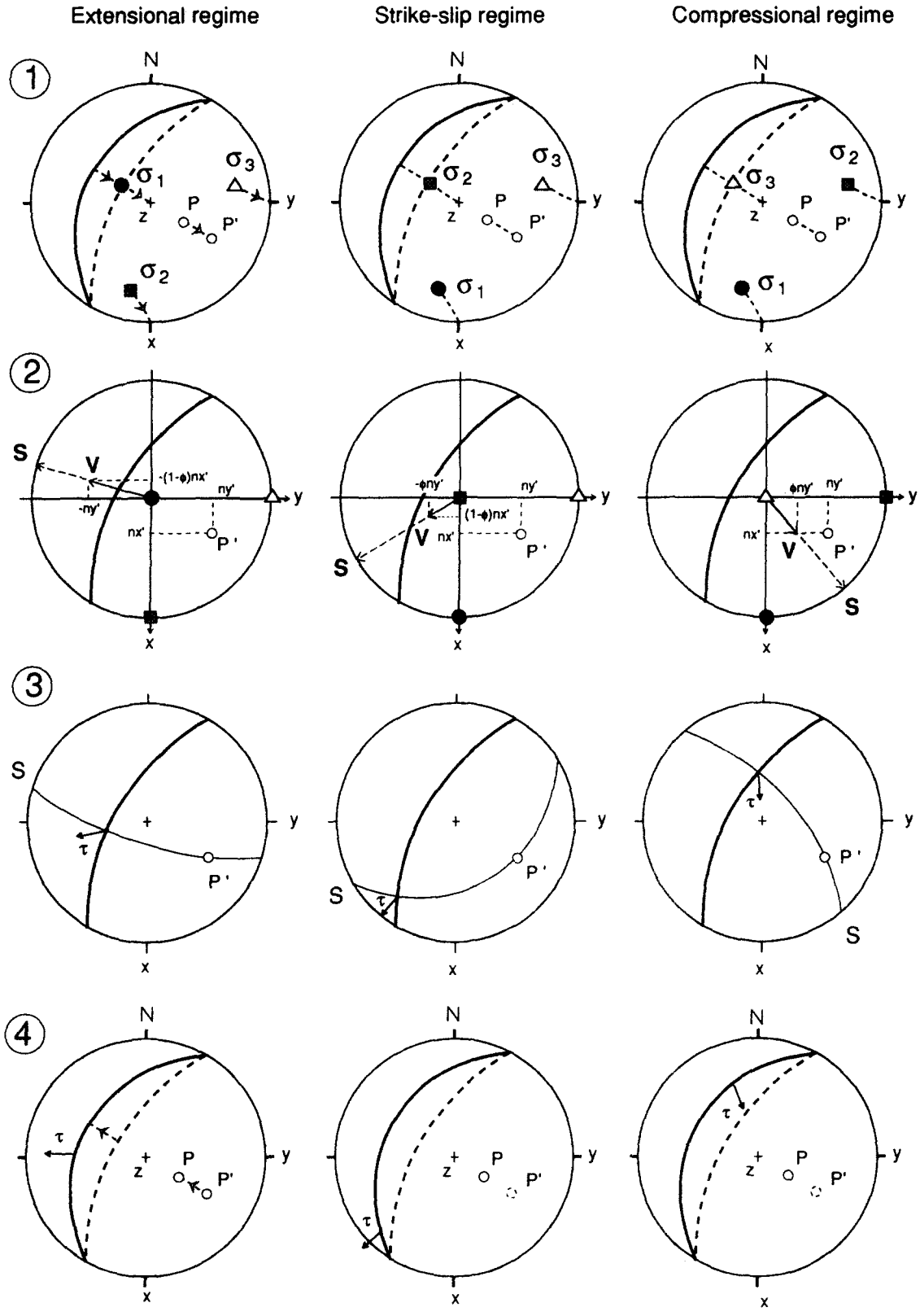

Fig. 2. Graphical determination using a stereographic projection (lower hemisphere) of the slip vector on a given fault plane from the reduced stress tensor expression, for the three main tectonic stress regimes. (1) Rotation of the fault plane and its pole in order to bring back to vertical one of the three principal stress axes according to the considered stress regime. (2) Construction of the horizontal vector **V** that is parallel to the resolved stress vector **S** applied to the fault plane. (3) Construction of the slip vector τ (parallel to the shear stress) applied to the fault plane by determining the plane which passes through the vector **S** and the fault pole **P'**. (4) Rotation of the fault plane back to the initial position. Note that in the actual examples, the required rotations in steps (1) and (4), will not generally be rotations about the fault strike direction as rotation axis.

plane with the fault plane gives the direction of τ. Its sense is the same as vector **S**.

(4) The calculated slip vector τ and the fault plane are rotated back to the initial reference frame (Fig. 2, stage 4). This last rotation is opposite to the one made during the first operation.

CONCLUSIONS

The classification of stress states and the graphical method for slip vector construction that have been presented are based on a simplification of the stress tensor expression such that its components only depend on the stress ratio $\phi = (\sigma_2 - \sigma_3)/(\sigma_1 - \sigma_3)$. Using this definition and assuming Andersonian stress states (one of the principal stress axes is vertical), compressional, strike-slip and extensional regimes have been treated separately.

Among the other existing graphical methods which enable one to determine the direction of shear on a given fault surface, the stereographic construction presented in this paper has similarities with those published by Means (1989), Ragan (1990) Fleischmann (1992) and Fry (1992). Its main difference is the choice of subtracting σ_z instead of σ_2 as the magnitude of the isotropic component in the stress reduction. Nevertheless, the present graphical method is the only one other than De Paor's (1990), which can be performed entirely by hand with only two simple multiplications. All the other methods require trigonometric calculations (Lisle 1989, Means 1989, Ragan 1990, Fleischmann 1992, Fry 1992). From that point of view, it can easily be applied in the field and is therefore useful for geologists. For instance, it enables the prediction of the slip direction on large faults around which the stress state is known.

Acknowledgements—I would like to thank A. Etchecopar, M. Mattauer, H. Philip, A. Taboada, B. Célérier, J. Jackson, A. Smith and C. Baker for fruitful discussions, and N. Fry, W. D. Means and S. H. Treagus who reviewed and improved the manuscript with their helpful comments and suggestions.

REFERENCES

Anderson, E. M. 1951. *The Dynamics of Faulting*. Oliver and Boyd, Edinburgh.

Angelier, J. 1975. Sur l'analyse de mesures recueillies dans des sites faillés: L'utilité d'une confrontation entre les méthodes dynamiques et cinématiques. *C. r. Acad. Sci., Paris* **281**, 1805–1808.

Bott, M. H. P. 1959. The mechanics of oblique slip faulting. *Geol. Mag.* **96**, 109–117.

De Paor, D. G. 1990. The theory of shear stress and shear strain on planes inclined to the principal directions. *J. Struct. Geol.* **12**, 923–927.

Etchecopar, A. 1984. Etude des états de contraintes en tectonique cassante et simulations de déformations plastiques (approche mathématique). Unpublished Thèse d'Etat, Montpellier.

Fleischmann, K. H. 1992. A graphical construction for the shear stress on a fault surface. *J. Struct. Geol.* **14**, 499–502.

Fry, N. 1992. Direction of shear. *J. Struct. Geol.* **14**, 253–255.

Lisle, R. J. 1989. A simple construction for shear stress. *J. Struct. Geol.* **11**, 493–495.

Means, W. D. 1989. A construction for shear stress on a generally-oriented plane. *J. Struct. Geol.* **11**, 625–627.

Ragan, D. M. 1990. Direction of shear. *J. Struct. Geol.* **12**, 929–931.

Wallace, R. E. 1951. Geometry of shearing stress and relation to faulting. *J. Geol.* **59**, 118–130.